Electronic Supplementary Material (ESI) for ChemComm.

Supporting Information

Specific extraction of nucleic acids employing pillar[6]arenes functionalized nanochannels platform

Yu Li[a,b], Wenjie Li [b], Weiwei Xu[b], Jinmei Huang[b], Zhongyue Sun[c,*], Tangbin Liao[d,*], Elena G. Kovaleva[e], Chuanlai Xu[a,*], Jing Cheng[b,*] and Haibing Li[b,*]

a. State Key Laboratory of Food Science and Technology, Jiangnan University.

b. Key Laboratory of Pesticide and Chemical Biology (CCNU), Ministry of Education, College of Chemistry, Central China Normal University, Wuhan 430079, P. R. China.

c. School of Laboratory Medicine, Hubei University of Chinese Medicine, Wuhan 430065, P.R. China.

d. School of Pharmacy, Hubei University of Chinese Medicine, Wuhan 430065, P.R. China.

e. Department of Technology for Organic Synthesis, Ural Federal University, Mira Street, 28, 620002 Yekaterinburg, Russia.

Table of contents

1. Materials

Poly ethylene terephthalate (PET, 12 μm thick) membranes were irradiated with Au ions of 11.1 MeV/nucleon kinetic energy at the UNILAC linear accelerator (GSI, Darmstadt, Germany). 1-Ethyl-3-(3-dimethyllaminopropyl) carbodiimide hydrochloride (EDC • HCl, ≥98.5%), N-Hydroxysuccinimide (NHS, ≥98.0%), sodium hydroxide, hydrochloric acid, formic acid, potassium chloride, sodium hydrogen phosphate, sodium dihydrogen phosphate, boric acid, o-Phthalaldehyde (OPA), methanol, mercaptoethanol, ethidium bromide (EB) were purchased from Sinopharm Chemical Reagent Shanghai Co. Ltd. lysine (Lys), valine (Val), histidine (His), leucine (Leu), isoleucine (Ile), methionine (Met), phenylalanine (Phe), threonine (Thr), tryptophan (Trp), Lysozyme (LZ)，and bovine serum albumin (BSA) were obtained from Energy Chemical. Escherichia coli pathogenic gene, a fragment of the eaeA gene (5'-GTC ACA GTT GCA GGC CTG GTT ACA ACA TTA TG-3') (NCBI: AF081182.1), purchased from Sangon Bioengineering. The reagents used have not been processed before being used. All chemical reagents were prepared in deionized water (18.2 MΩ). Current-voltage curves were measured by a Keithley 6487 picoammeter (Keithley Instruments, Cleveland, OH). Scanning electron microscope (SEM) was obtained with a JSM-6700F system of Japan. Confocal fluorescent images were acquired using a Zeiss confocal laser scanning unit mounted on an LSM710 fixed-stage upright microscope.

2. Synthesis of Gly-P6

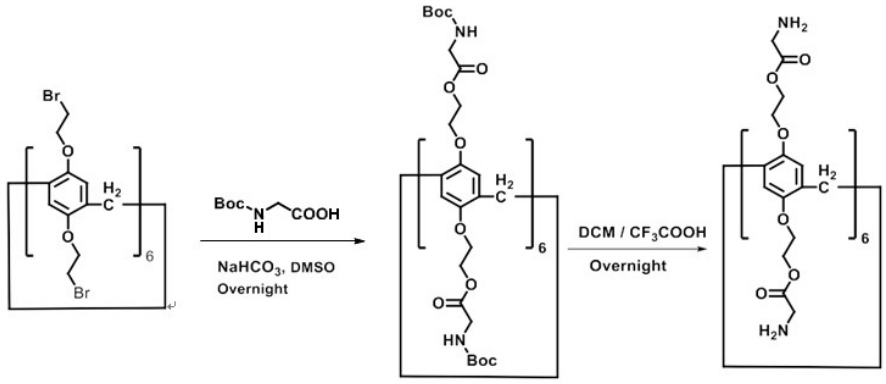

Scheme S1. The preparation of Gly-P6.

Note S1. Synthesis of Gly-P6

Boc-Gly-P6 was synthesized by our group, and its ^{1}H NMR (600 MHz, DMSO-*d6*) data was δ (ppm): 7.22 (d, 12H, Boc-NH), 6.70 (s, 12H, Ar-H), 4.43 (s, 12H, NH-CH), 4.25 (s, 12H, NH-CH), 3.99 (s, 12H, Ar-CH_2), 3.70 (m, 48H, Ar-O-CH_2-CH_2), 1.36 (s, 108H, NH-Boc). The next step is to remove the Boc protection group. 200 mg Boc-Gly-P6 was placed in a 50 mL round-bottom flask, and the solvent mixture of 20 mL dichloromethane and trifluoroacetic acid was added. The reaction was carried out at room temperature under nitrogen protection for 12h. After the reaction, the solvent was removed by the evaporator, and the residue was recrystallized with methanol/ether. After standing for 6 h, the solution was poured out and dried in a vacuum. The light yellow solid was 164 mg with a yield of 78.1%. ^{1}H NMR (600 MHz, MeOH-*d6*), δ(ppm): 6.73 (s, 12H, Ar-H), 4.46 (s, 24H, NH-CH), 4.02 (s, 24H, NH-CH), 3.76 (s, 12H, Ar-CH_2), 3.86 (m, 24H, Ar-O-CH_2-CH_2). .Gly-P6 calcd for m/z :1944.79, found: 1946.36.

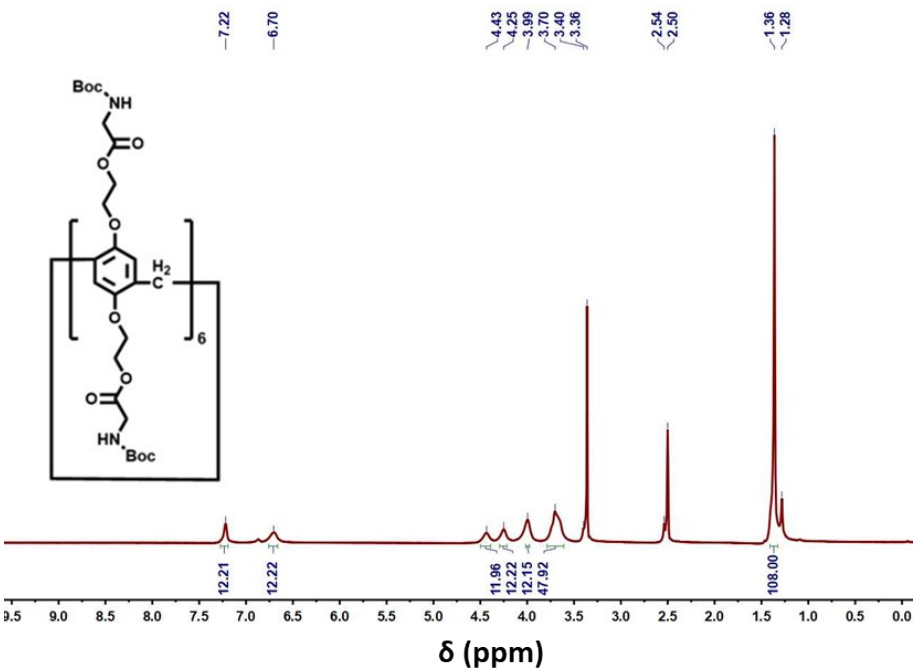

Figure S1. [1]H NMR spectrum of Boc-Gly-P6 (600 MHz, DMSO-*d6*, 298 K).

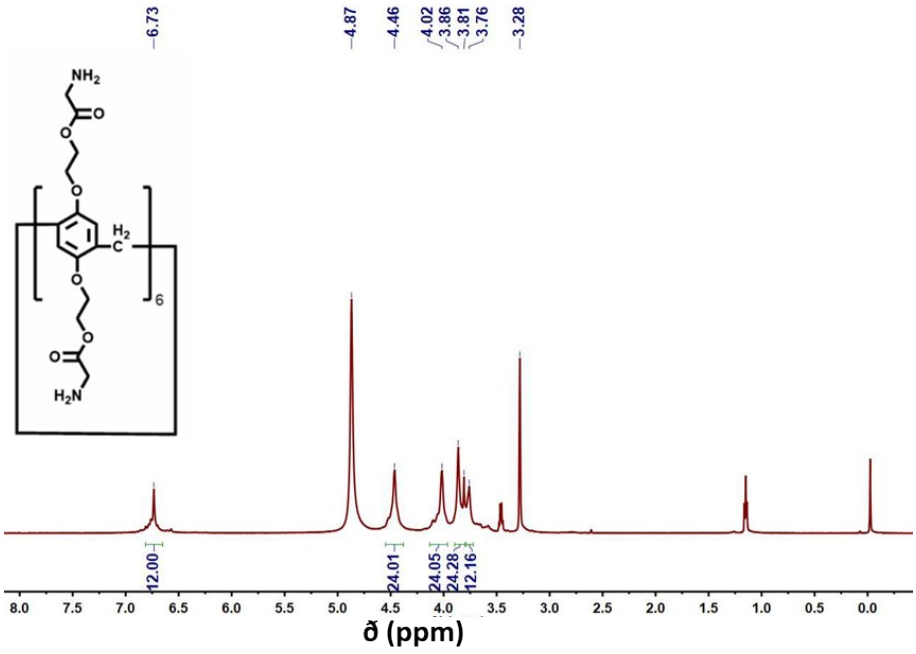

Figure S2. [1]H NMR spectrum of Gly-P6 (600 MHz, MeOH-*d6*, 298 K).

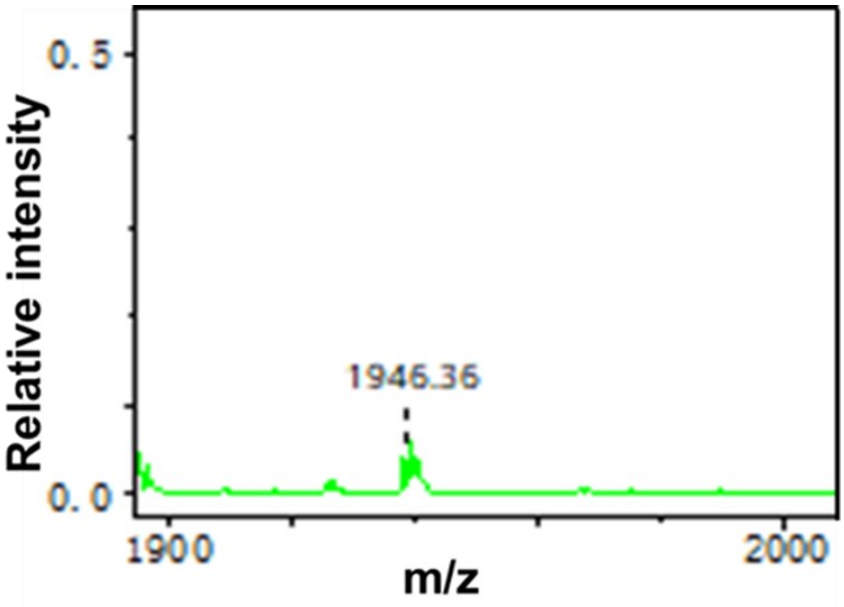

Figure S3. Mass spectrometric characterization of Gly-P6

3. Synthesis of the monomer of glycine pillar[6]arene (Gly-mo)

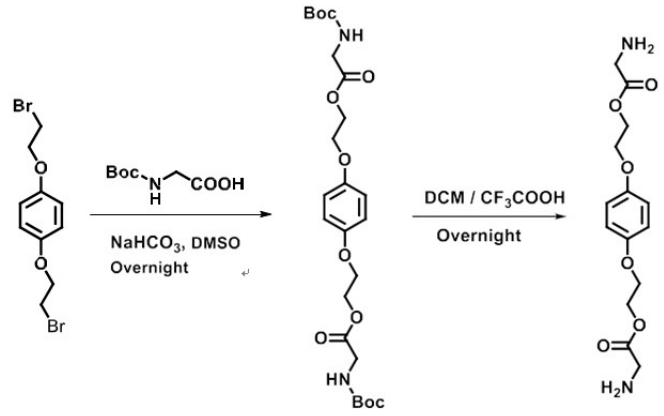

Scheme S2. The preparation of Gly-mo.

Note S2. Synthesis of Gly-mo

First, Boc-glycine monomer needed to be synthesized. Bromide monomer (50 mg, 0.15 mmol), Boc-glycine monomer (540.6 mg, 3.086 mmol) and sodium bicarbonate (295.25 mg, 3.086 mmol) were placed in a 50 mL round-bottomed flask. 25 mL dimethyl sulfoxide (DMSO) solution was added, and reacted at 50 ^{o}C for 12 h under the protection of nitrogen. After the reaction, the white solid was obtained by post-treatment in the same way as that of Gly-P6. The product was weighed

83 mg with a yield of 63.8%. After removing the Boc protector, a light yellow solid of 58 mg was obtained with a yield of 74.1%. ^{1}H NMR (400 MHz, MeOH-d_6) data is δ (PPM): 6.78 (s, 4 H, Ar - H), 4.47 (t, 4 H, Ar - O - CH_2), 4.08 (t, 4 H, Ar - O - CH_2 - CH_2), 3.76 (s, 4 H, NH - CH).

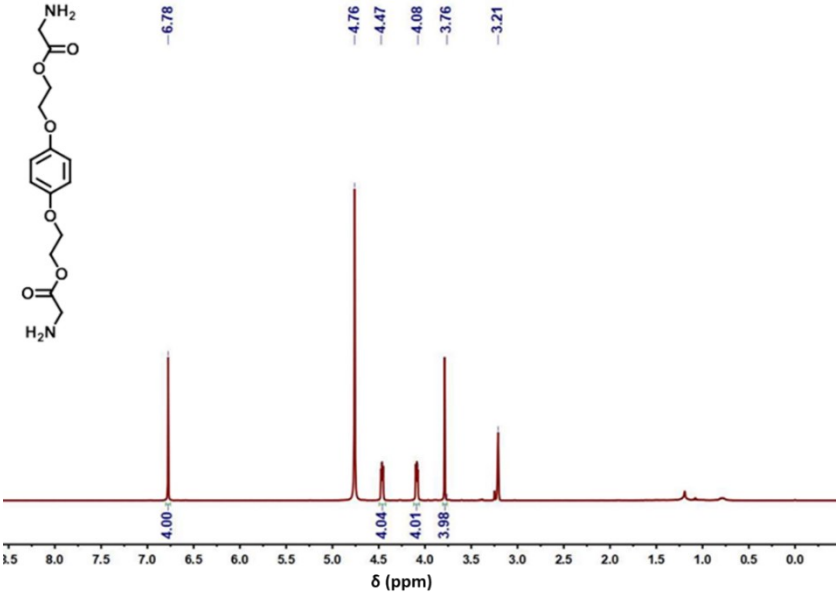

Figure S4.^{1}H NMR spectrum of Gly-mo (400 MHz, MeOH-d_6, 298 K).

4. Nanochannels fabrication

The conical nanochannels were prepared in Poly ethylene terephthalate (PET) membrane using the ion track etching technique. Firstly, The PET film is placed under a UV lamp (365 nm) for one hour on both sides, and then chemically etched in the two chambers of the conductivity cell (the left side is full of 9 M NaOH as etching liquid, the right is full of 1 M HCOOH/KCl as prevent fluid). The etching is monitored at a voltage of DC=1 V, the etching is stopped when the current reaches the desired value, and the etching solution at both ends is removed and the blocking solution is added at the same time.

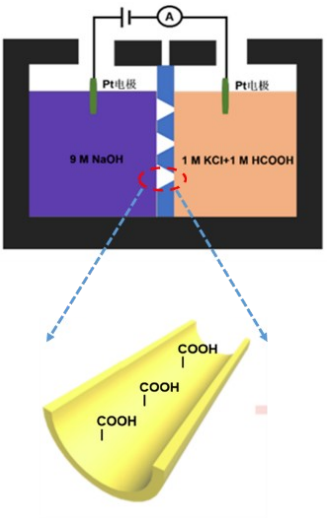

Figure S5. Schematic image for the etching process of nanochannels.

5. SEM characterization

The diameter of the large opening of the conical membrane channels denoted base, (D) was determined by scanning electron microscopy (SEM). The diameter of the small opening, denoted tip, tip (d_{tip}) was estimated by the following relation. The base diameter is about 500 nm, and the tip size is around 20 nm.

$$d_{\text{tip}} = \frac{4LI}{\pi\, k(c) U\, D}$$

L is the length of the pore, which could be approximated by the thickness of the membrane after chemical etching; I is the measured ion current; U is the applied voltage; d_{tip} and D is the tip diameter and the base diameter, respectively; k(c) is the specific conductivity of the electrolyte. For 1 M KCl solution at 25 °C, k(c) is 0.11173 Ω^{-1} cm^{-1}.

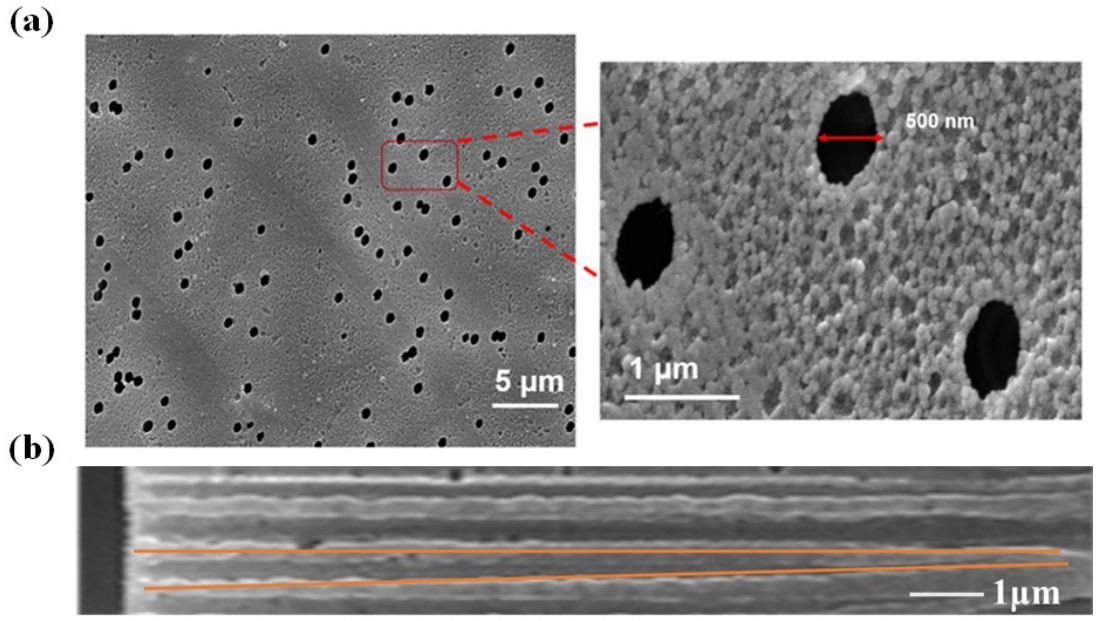

Figure S6. (a) Scanning electron microscopy (SEM) image of conical nanopores in track-etched PET membrane. The diameters of the large opening (Base) are approximately 500 nm. (b) Cross-section of the conical nanopore.

6. XPS analysis

Table S1. XPS data of PET film before modification

Bare	Peak BE	FWHM eV	Area(P) CPS.eV	Atomic %
C1s	284.62	1.84	147448.12	73.62
O1s	532.23	3.18	151303.23	26.38

Table S2. XPS data of PET film after modified with Gly-P6

Bare	Peak BE	FWHM eV	Area(P) CPS.eV	Atomic %
C1s	284.76	1.63	94882.09	75.27
N1s	399.74	1.79	7361.43	3.61
O1s	532.37	3.18	70448.06	21.12

7. ss DNA transport experiments in Gly-P6 channels

For the transport experiments, the prepared nanochannel membranes were mounted between the two halves of the conductivity cell. Each cell volume was 1.5 ml, and the feed cell (left side) contained 10^{-6} M ss DNA in 0.01 M PBS solution, whereas the permeate cell (right side) was filled with pure PBS solution. To monitor the entire transport process, we measured the flux rate of ss DNA transport by periodically assaying the permeate cell solution respectively using a fluorescence analysis method.

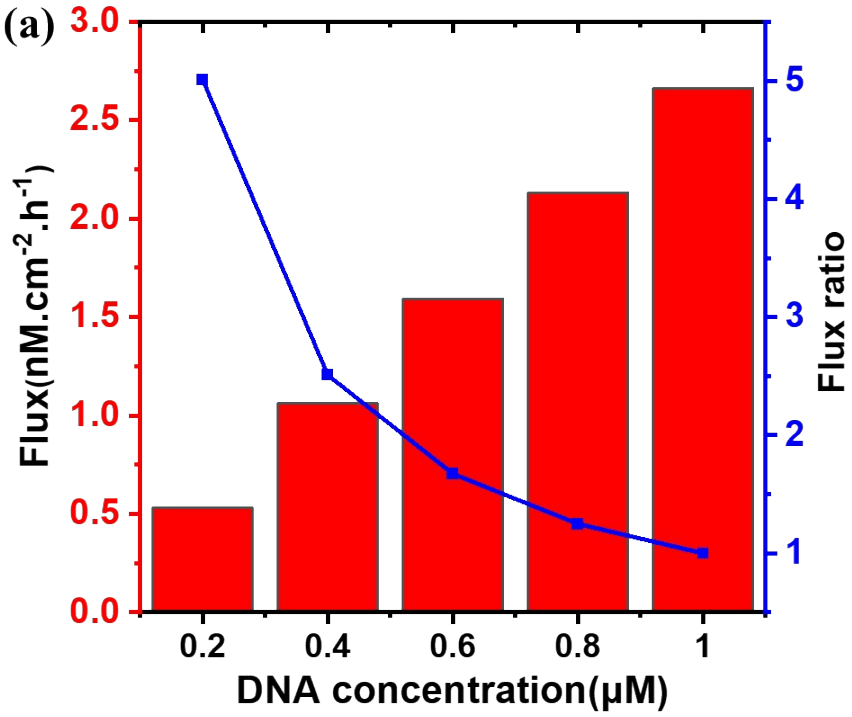

Figure S7. (a) Transport flux and flux ratio of ss DNA at different concentrations.

ss DNA has endogenous fluorescence, but its endogenous fluorescence intensity is very small and cannot be directly studied. EB can be used as a fluorescent probe, but its fluorescence intensity is also very small. However, when EB is added to ss DNA, the fluorescence intensity of the system is greatly enhanced, so in this experiment, EB (5×10^{-6} M) was used to label the ss DNA in the transfer solution.

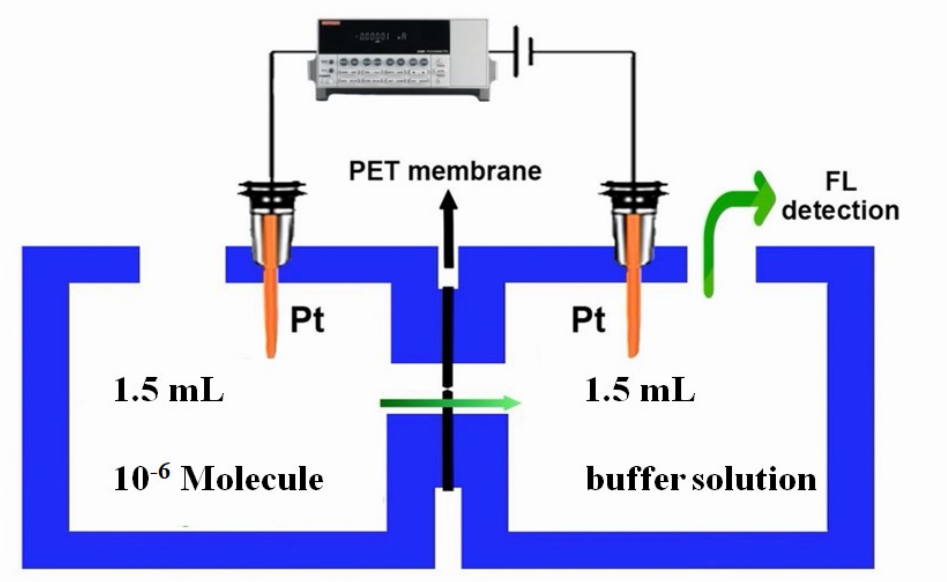

Figure S8. The schematic diagram of transport device for molecule.

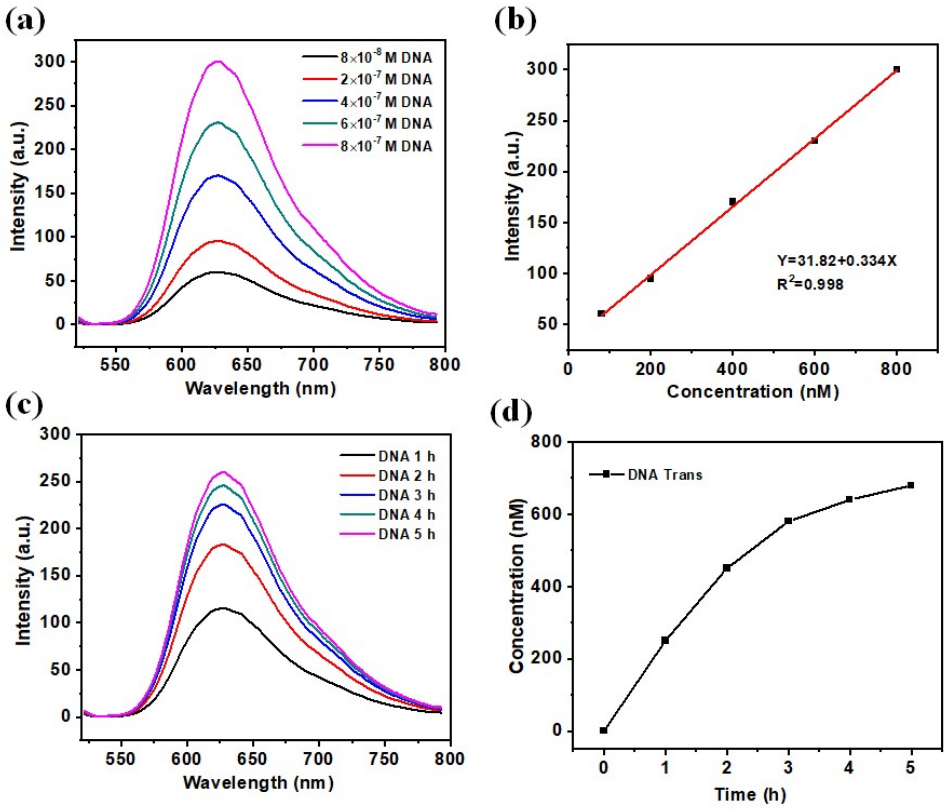

Figure S9. (a) Standard curve of ss DNA labeled with EB. (b) The relationship between fluorescence intensity and concentration of EB-labeled ss DNA. (c) Fluorescence spectroscopy characterizes the transmission behavior of ss DNA in Gly-P6 channels. (d) ss DNA transport flux in Gly-P6 modified nanochannels.

Hence, the flux of molecule can be calculated from the formula S1.

$$Flux\left(nmol \cdot m^{-2} \cdot h^{-1}\right) = \frac{VC}{St} \quad \text{.....S1}$$

V: the total volume of the receiving liquid after transport, V = 1.5 mL; S: the effective area of the membrane surface in the transport process S = 0.384 cm^2. C: The concentration of molecule in the receiving solution after transport and the transport time.

8. Lys transport experiments in Gly-P6 channels

The OPA derivatization method used in this experiment, in the borate buffer solution of pH = 9.5, OPA and mercaptoethanol react with amino acids to generate isoquinoline derivatives with strong fluorescence emission. Neither the amino acids nor the OPA derivatization reagent emits fluorescence, and strong fluorescence will only be generated after the combination of the amino acids and the OPA derivatization reagent.

OPA derivative method: first of all, 4.76 g borax was placed in 100 mL distilled water, which was completely dissolved by ultrasound to prepare 0.05 M borax solution. Then, OPA solution was prepared. 50 mg OPA was added to 1 mL methanol, which was completely dissolved by ultrasound. 500 μL mercaptoethanol was added, and then the solution was diluted to 10 mL with boric acid (pH = 9.5) buffer solution after uniform shaking. Finally, the derivatization experiment of amino acids was carried out. About 100 times the equivalent of OPA was added to the amino acid solution.

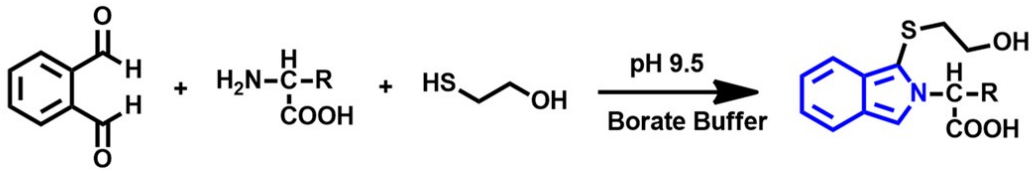

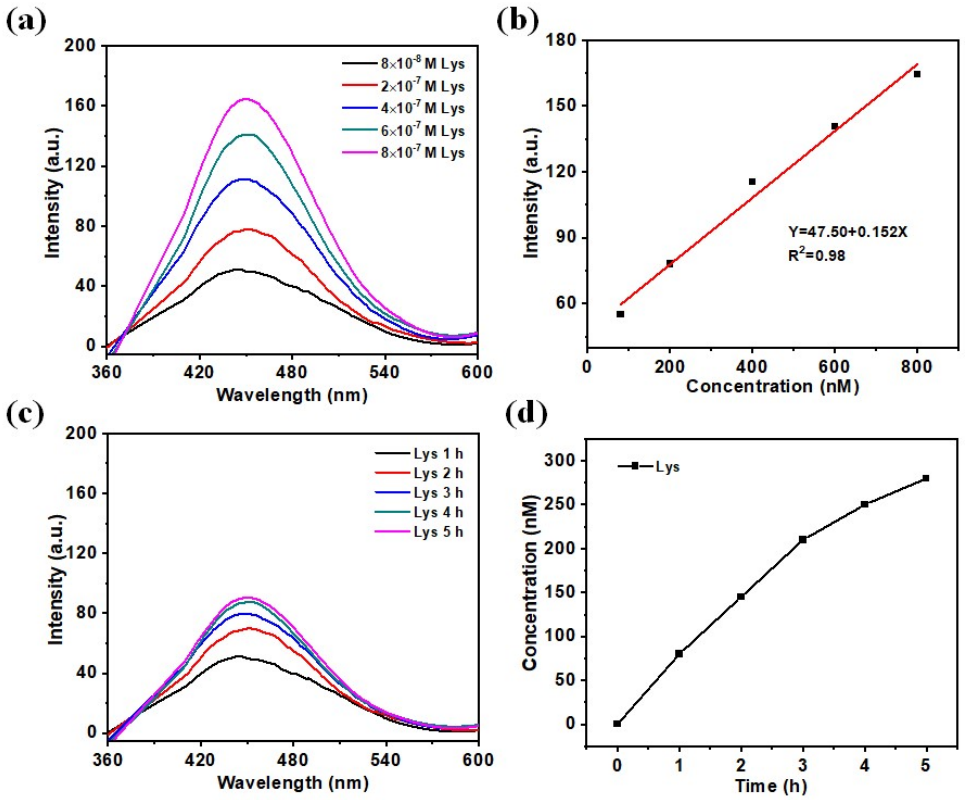

Figure S10. (a) Standard curve of Lys derivatized by OPA. (b) The relationship between fluorescence intensity and concentration of OPA-derived Lys. (c) Fluorescence spectroscopy characterizes the transmission behavior of Lys in Gly-P6 channels. (d) Lys transport flux in Gly-P6 modified nanochannels.

9. Val transport experiments in Gly-P6 channels

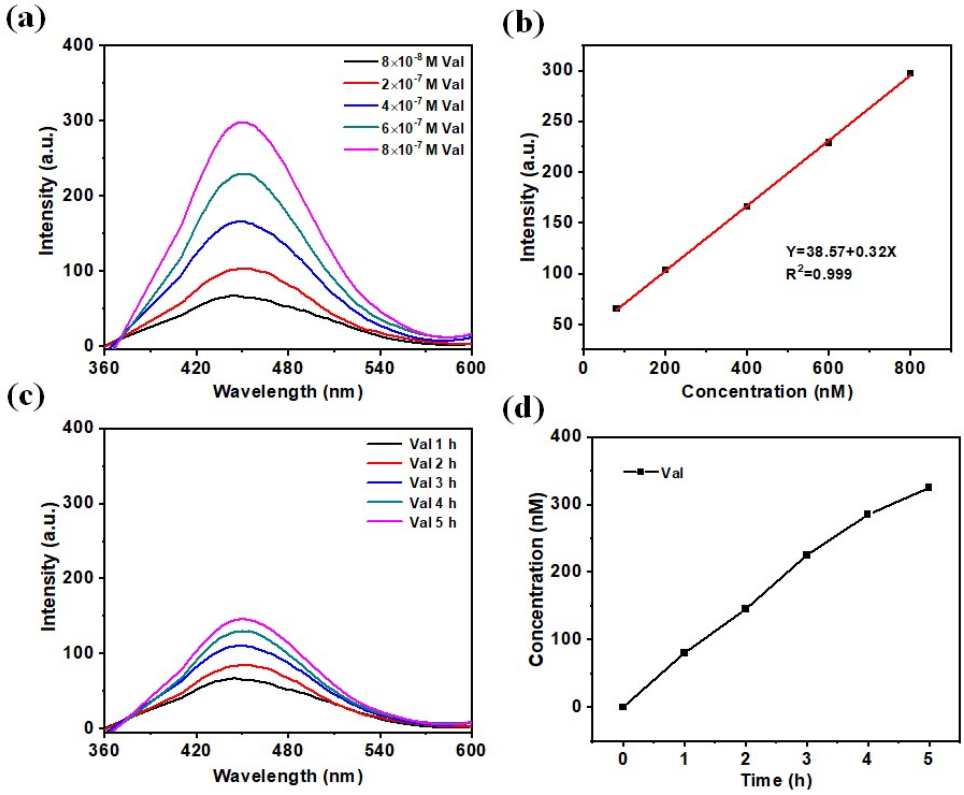

Figure S11. (a) Standard curve of val derivatized by OPA. (b) The relationship between fluorescence intensity and concentration of OPA-derived val. (c) Fluorescence spectroscopy characterizes the transmission behavior of val in Gly-P6 channels. (d) Val transport flux in Gly-P6 modified nanochannels.

10. His transport experiments in Gly-P6 channels

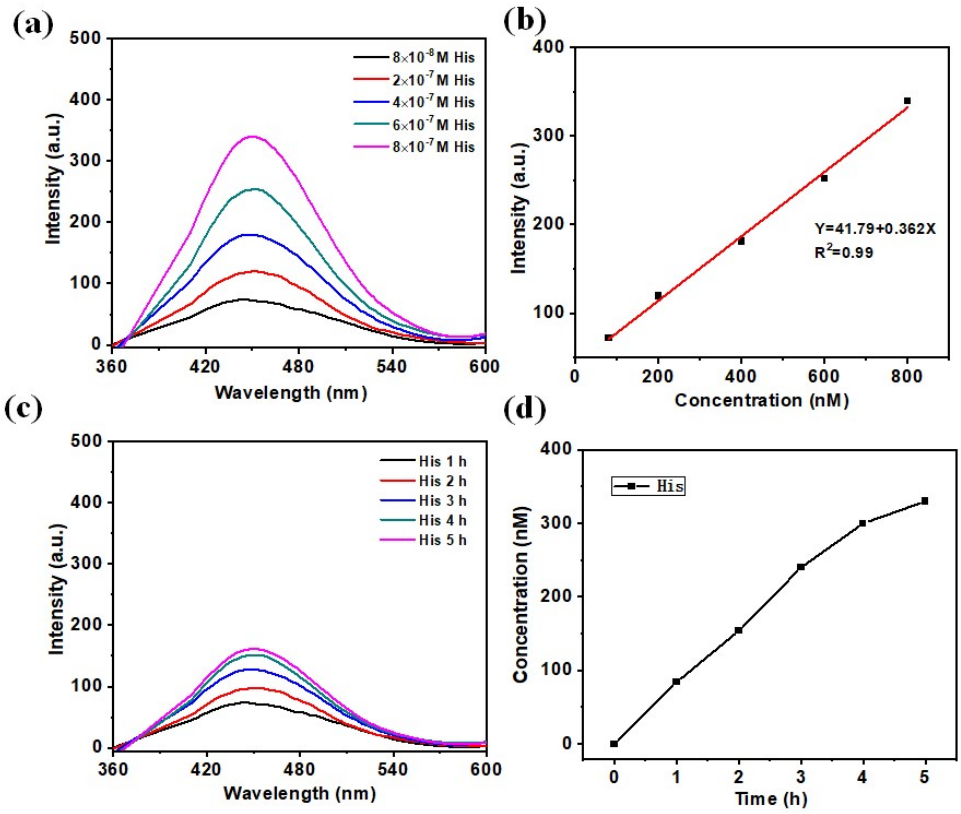

Figure S12. (a) Standard curve of His derivatized by OPA. (b) The relationship between fluorescence intensity and concentration of OPA-derived His. (c) Fluorescence spectroscopy characterizes the transmission behavior of His in Gly-P6 channels. (d) His transport flux in Gly-P6 modified nanochannels.

11. Leu transport experiments in Gly-P6 channels

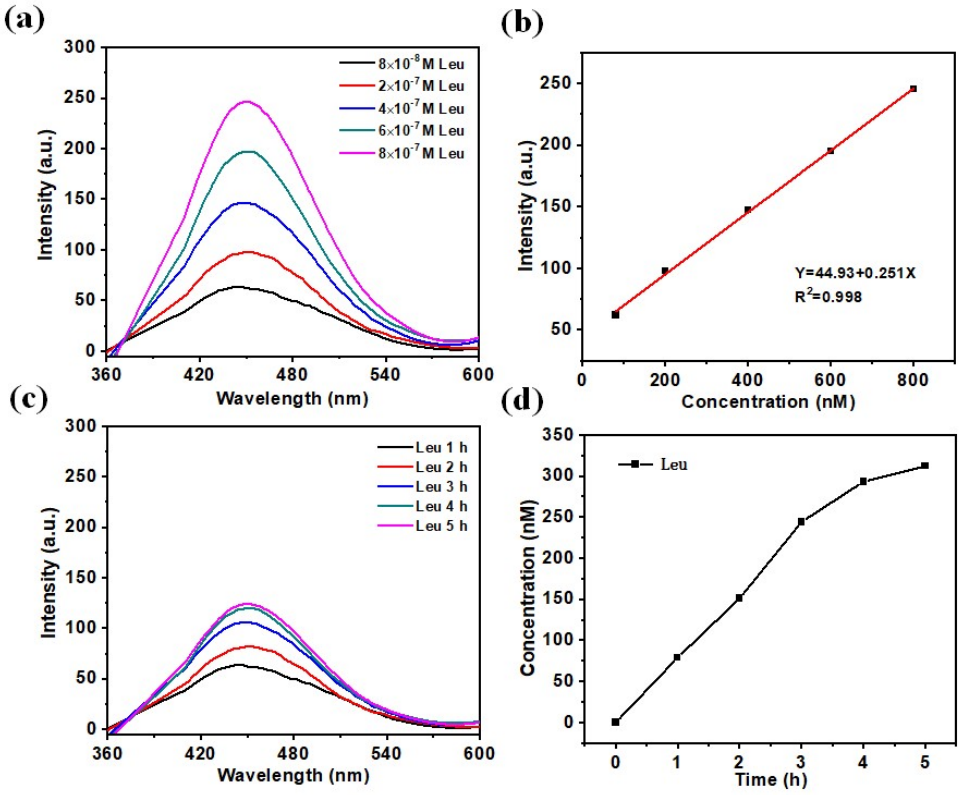

Figure S13. (a) Standard curve of leu derivatized by OPA. (b) The relationship between fluorescence intensity and concentration of OPA-derived leu. (c) Fluorescence spectroscopy characterizes the transmission behavior of leu in Gly-P6 channels. (d) Leu transport flux in Gly-P6 modified nanochannels.

12. Ile transport experiments in Gly-P6 channels

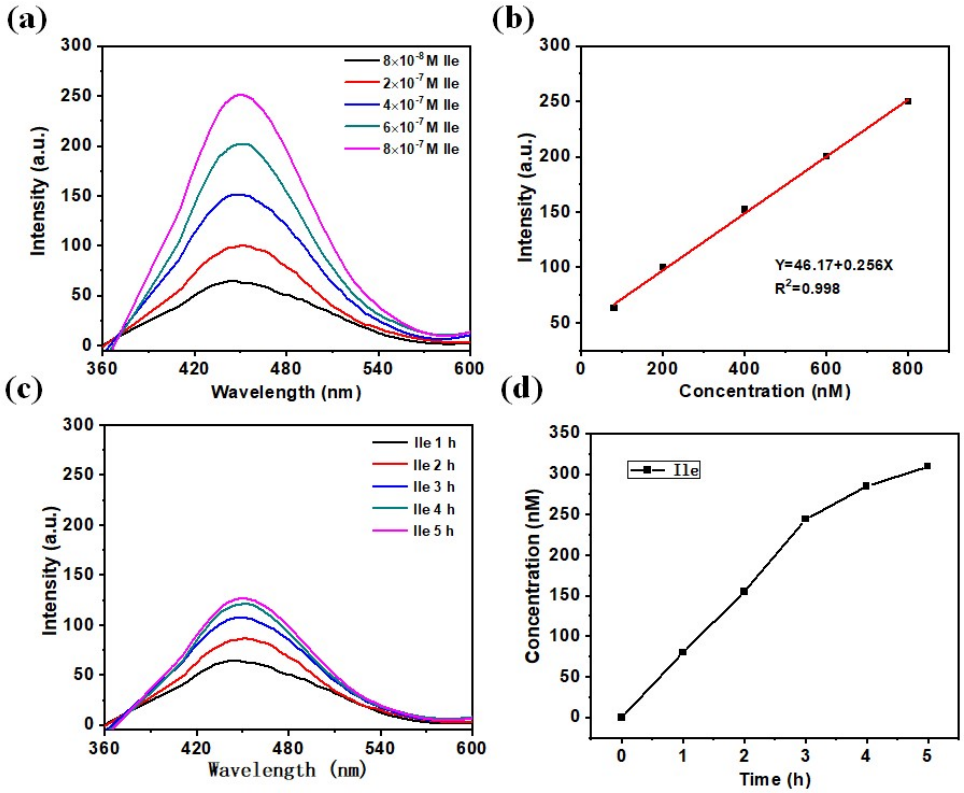

Figure S14. (a) Standard curve of Ile derivatized by OPA. (b) The relationship between fluorescence intensity and concentration of OPA-derived Ile. (c) Fluorescence spectroscopy characterizes the transmission behavior of Ile in Gly-P6 channels. (d) Ile transport flux in Gly-P6 modified nanochannels.

13. Met transport experiments in Gly-P6 channels

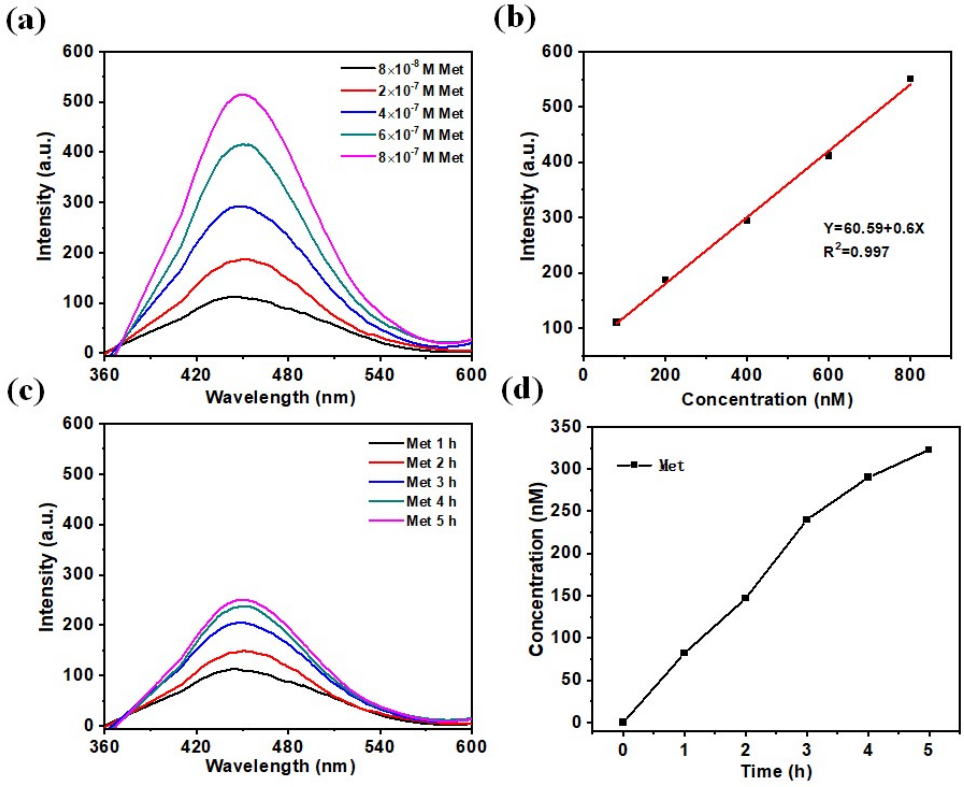

Figure S15. (a) Standard curve of Met derivatized by OPA. (b) The relationship between fluorescence intensity and concentration of OPA-derived Met. (c) Fluorescence spectroscopy characterizes the transmission behavior of Met in Gly-P6 channels. (d) Met transport flux in Gly-P6 modified nanochannels.

14. Phe transport experiments in Gly-P6 channels

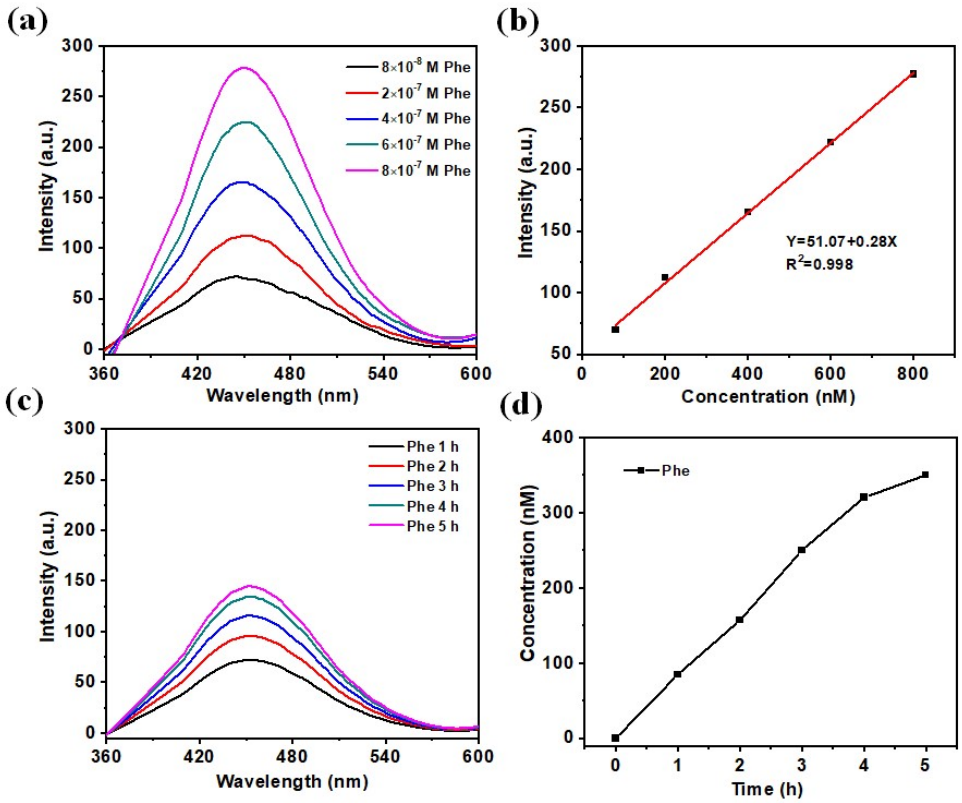

Figure S16. (a) Standard curve of Phe derivatized by OPA. (b) The relationship between fluorescence intensity and concentration of OPA-derived Phe. (c) Fluorescence spectroscopy characterizes the transmission behavior of Phe in Gly-P6 channels. (d) Phe transport flux in Gly-P6 modified nanochannels.

15. Thr transport experiments in Gly-P6 channels

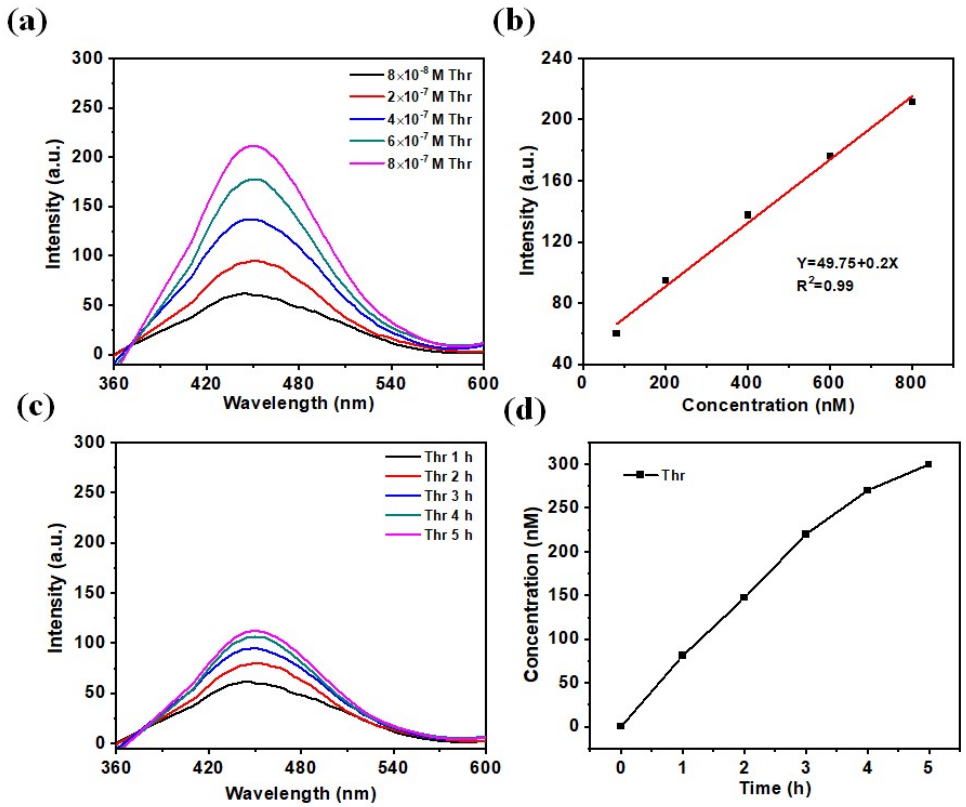

Figure S17. (a) Standard curve of Thr derivatized by OPA. (b) The relationship between fluorescence intensity and concentration of OPA-derived Thr. (c) Fluorescence spectroscopy characterizes the transmission behavior of Thr in Gly-P6 channels. (d) Thr transport flux in Gly-P6 modified nanochannels.

16. Trp transport experiments in Gly-P6 channels

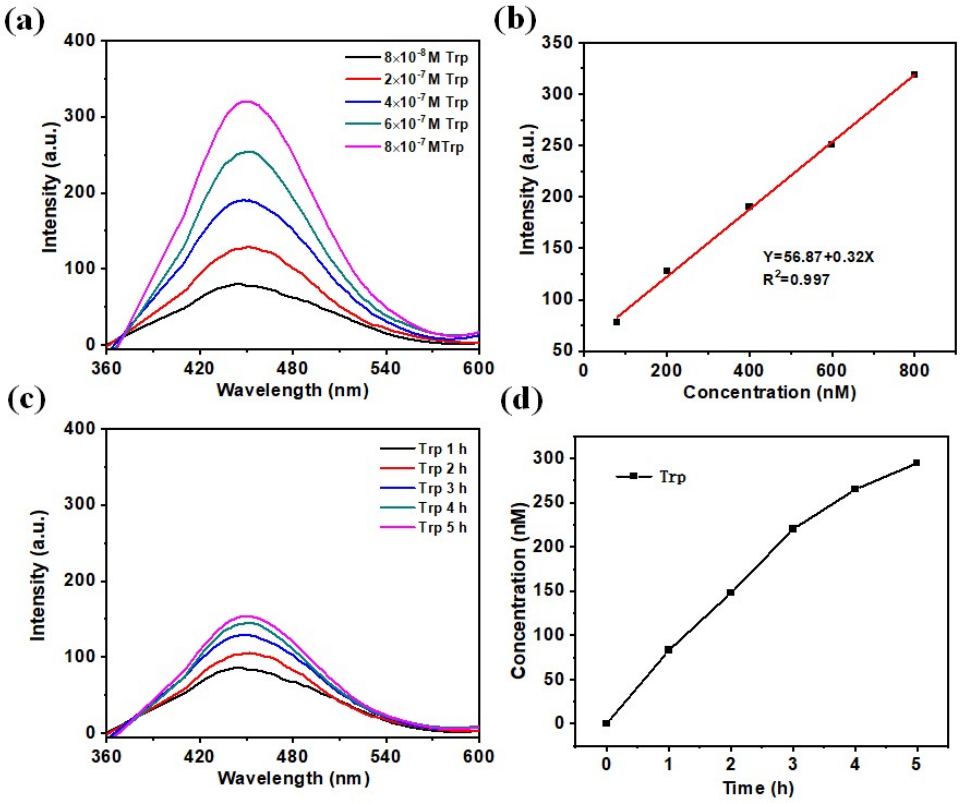

Figure S18. (a) Standard curve of Trp derivatized by OPA. (b) The relationship between fluorescence intensity and concentration of OPA-derived Trp. (c) Fluorescence spectroscopy characterizes the transmission behavior of Trp in Gly-P6 channels. (d) Trp transport flux in Gly-P6 modified nanochannels.

17. BSA transport experiments in Gly-P6 channels

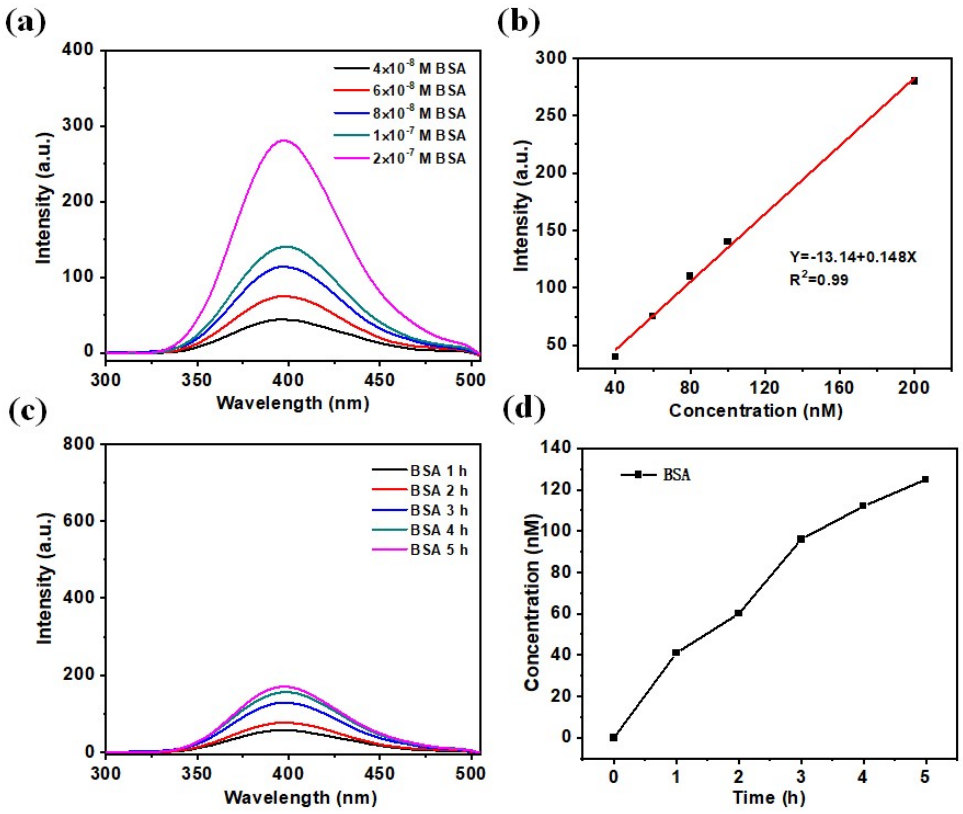

Figure S19. (a) Standard curve of BSA. (b) The relationship between fluorescence intensity and concentration of BSA. (c) Fluorescence spectroscopy characterizes the transmission behavior of BSA in Gly-P6 channels. (d) BSA transport flux in Gly-P6 modified nanochannels.

18. LZ transport experiments in Gly-P6 channels

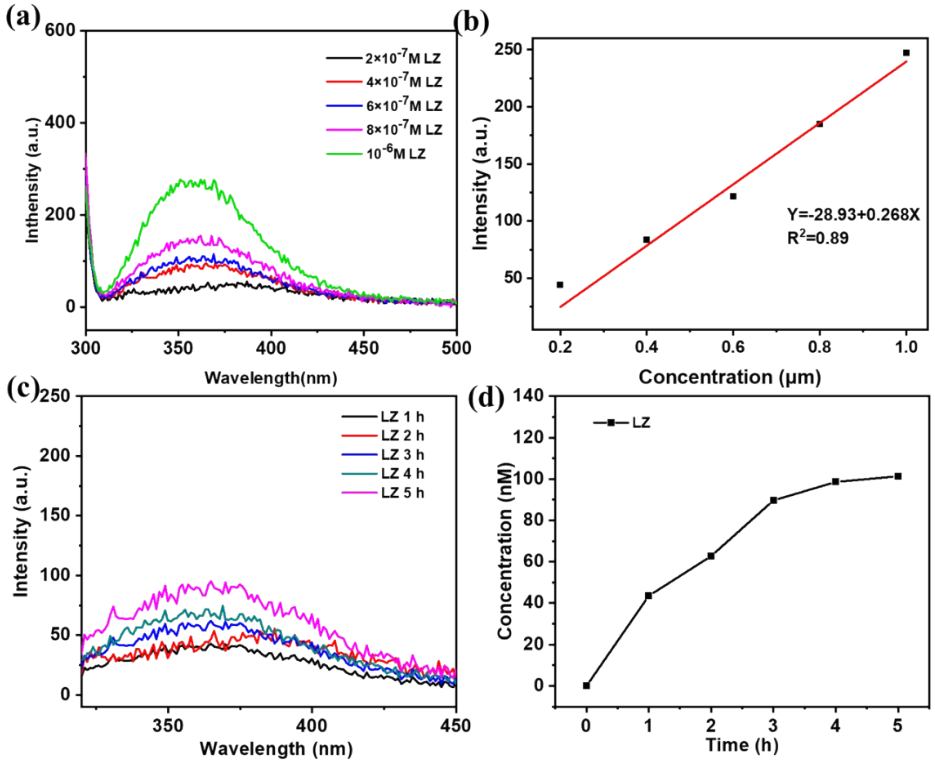

Figure S20. (a) Standard curve of LZ. (b) The relationship between fluorescence intensity and concentration of LZ. (c) Fluorescence spectroscopy characterizes the transmission behavior of LZ in Gly-P6 channels. (d) LZ transport flux in Gly-P6 modified nanochannels.

19. XPS characterization after transporting ss DNA

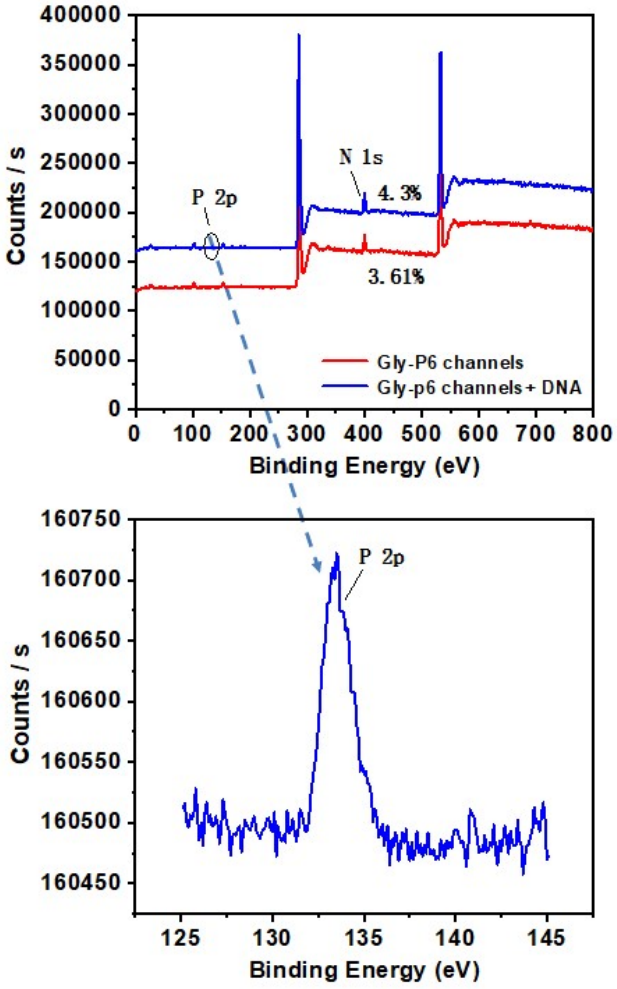

Figure S21. XPS spectra analysis of Gly-P6 channels before and after ss DNA transmission.

Table S3. XPS spectra analysis of Gly-P6 channels before and after ss DNA transmission.

Bare	Peak BE	FWHM eV	Area(P) CPS.eV	Atomic %
P2p	133.46	1.88	444.21	0.24
C1s	284.83	1.66	93065.11	72.03
N1s	399.86	1.89	8977.56	4.3
O1s	532.45	2.76	80119.55	23.43

20. Contact angle measurement

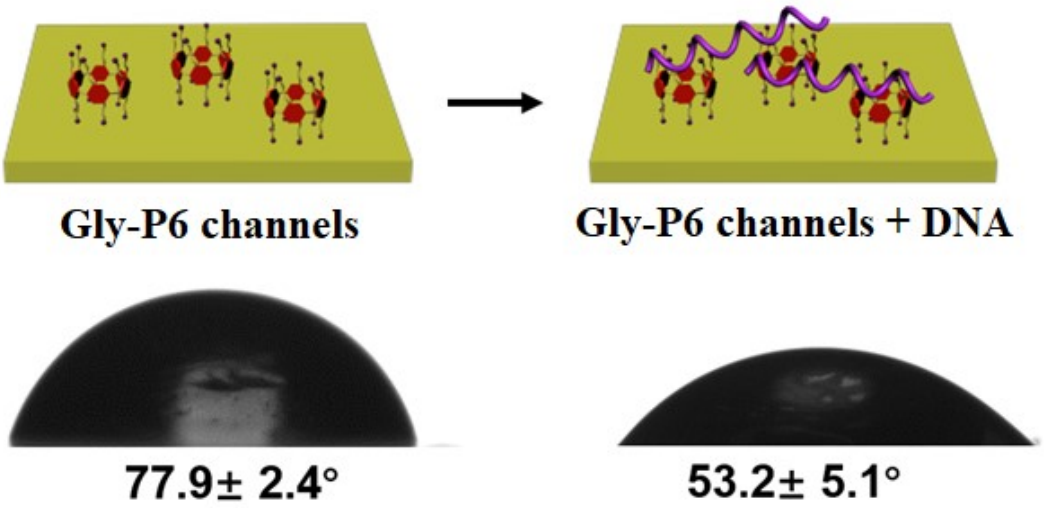

Figure S22. Contact angle of Gly-P6 channels before and after ss DNA transmission.

21. I-V current characterization for Gly-mo modified into the channels

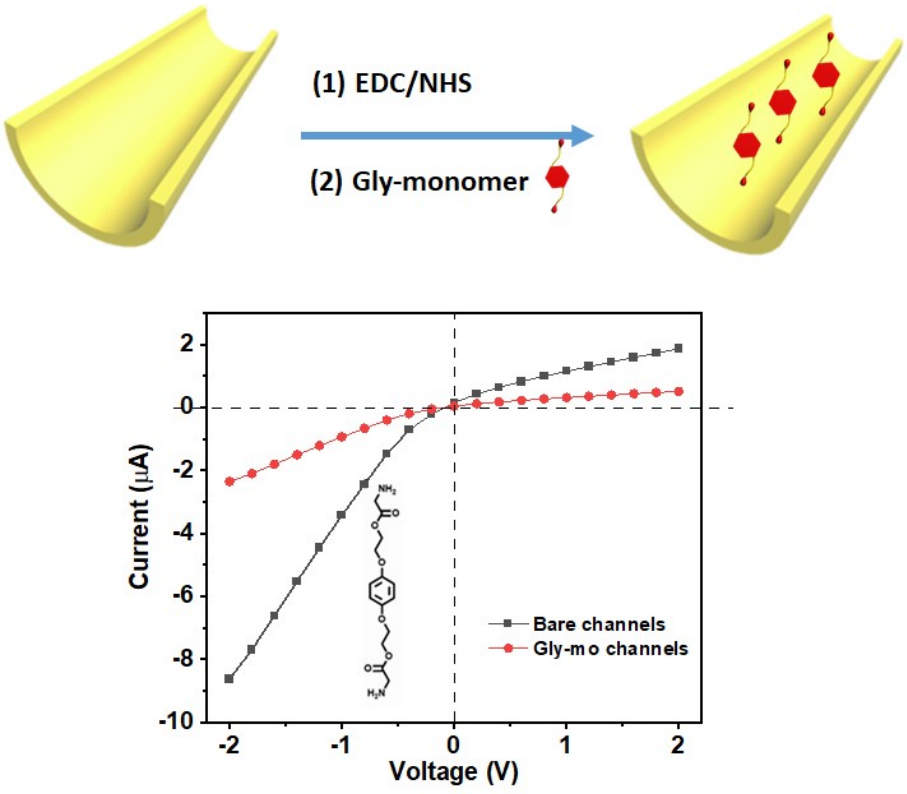

Figure S23. I-V current characterization for Gly-mo modified into the channels.

22. Ultraviolet-visible (UV-Vis) spectrum titration experiment with the interaction of Gly-P6 and Gly-mo with ss DNA

A 3 mL of 1 μM ss DNA solution was prepared, and the UV absorbance of the molecular solution was tested by UV-Vis spectroscopy. 0.2 times equivalent GLy-P6 and Gly-mo (0.1mM) were respectively added, and finally 1.8 times equivalent was added to test the UV absorbance change of ss DNA molecular solution.

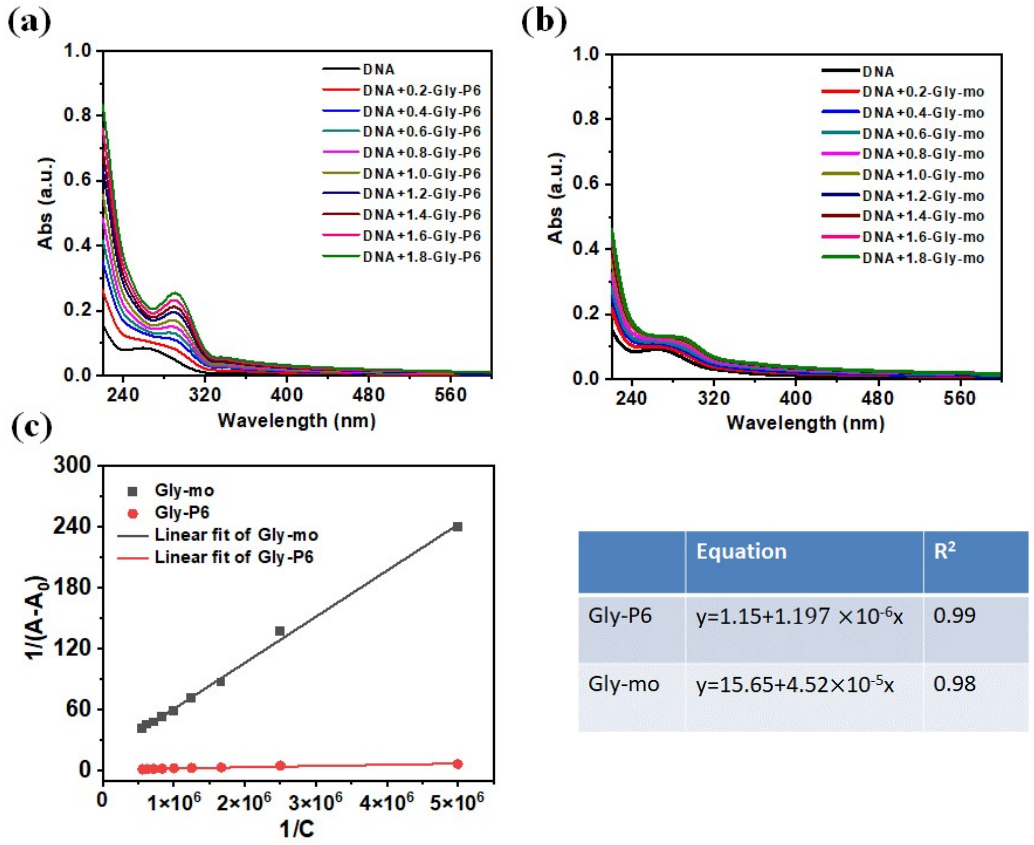

	Equation	R^2
Gly-P6	$y=1.15+1.197\times10^{-6}x$	0.99
Gly-mo	$y=15.65+4.52\times10^{-5}x$	0.98

Figure S24. 0, 0.2, 0.4, 0.6, 0.8, 1, 1.2, 1.4, 1.6, and 1.8 times equivalent of Gly-P6 (0.1mM) (a) and Gly-mo (0.1mM) (b) were added to 1 μM ss DNA solution in turn, and the absorbance changes were tested by UV-Vis spectroscopy; (c) The binding constants of ss DNA with Gly-P6 and Gly-mo were calculated by Benesi-Hilderbrand formula.

23. EOF test for the density of surface charge in channels

The mechanism of nucleic acid extraction was further confirmed by a series of electroosmotic flow (EOF) experiments. Phenol, which served as an electrically neutral probe, is used for measuring the EOF rate from the feed to the permeate. For the EOF experiment measurements, one side of the electrolytic cell was injected with the mixture solution of phenol (0.01 M) in PBS electrolyte solution (pH = 7.38). The other side only contained PBS electrolyte solution (0.01 M PBS, pH = 7.38). A fixed voltage was exerted on both sides, namely the permeated solution and the feed solution. The transport processes were monitored by fluorescence spectrum, then the rate of transport in the presence of the applied voltage (N_i) and the rate of diffusion (N_{diff}) were calculated. The velocity of electroosmotic flow (V_{eof}) was calculated by the ratio of these two transport rates (E). Then the surface charge density was calculated according to the velocity of electroosmotic flow, the applied voltage and the electrolyte. Among them, D is the expansion coefficient of the phenol solution, and L is the thickness of the PET film about 12 μm. ε and η represent the dielectric constant and viscosity of the solution, respectively, $\varepsilon = 6.95 \times 10^{-10}$ c^2 $J^{-1}m^{-1}$, η = 0.890 cP. In addition, the measured resistivity ρ of the electrolyte solution is 2.23 KΩ · cm, and J_{app} is the current density in the nanochannels.

$$E = \frac{N_i}{N_{diff}} = \frac{Pe}{1 - e^{-Pe}} \qquad S2$$

$$V_{eof} = \frac{PeD}{L} \qquad S3$$

$$\sigma = -\frac{V_{eof}\eta}{J_{app}\rho\kappa^{-1}} \qquad S4$$

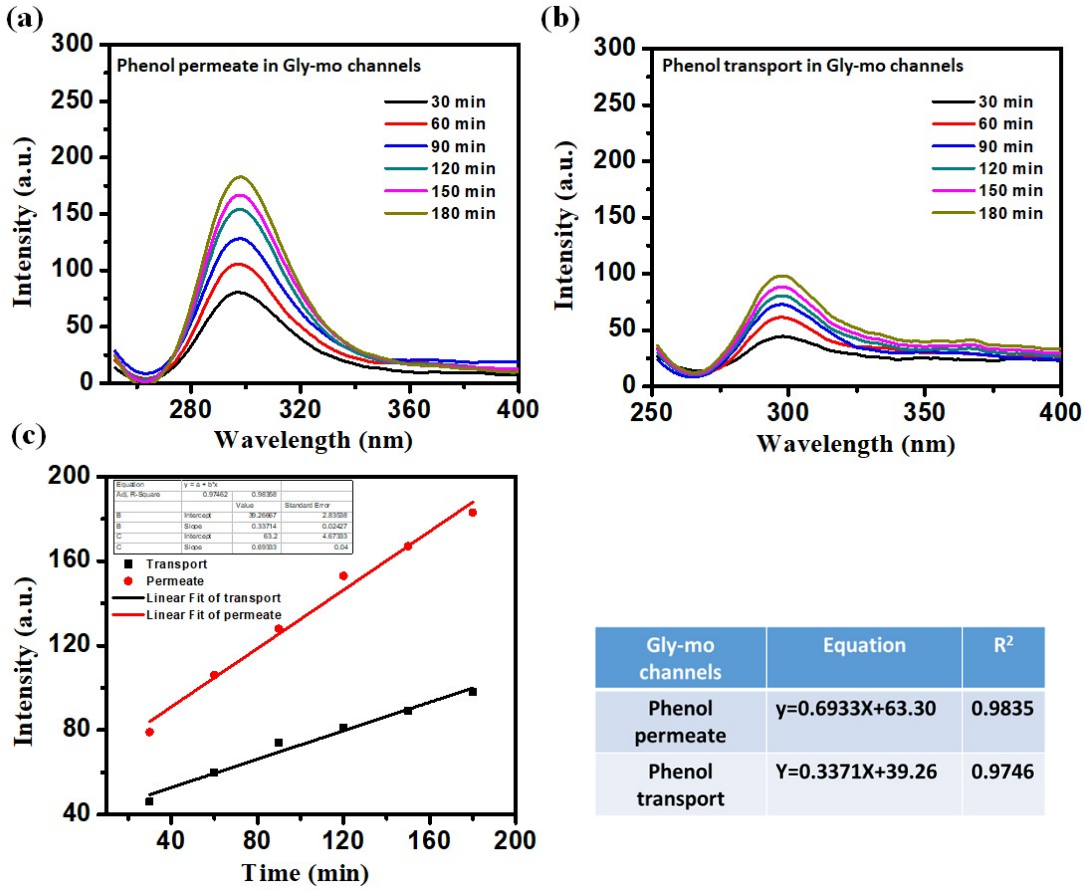

Gly-mo channels	Equation	R^2
Phenol permeate	y=0.6933X+63.30	0.9835
Phenol transport	Y=0.3371X+39.26	0.9746

Figure S25. (a) Fluorescence spectra of probe molecule (phenol) permeation in Gly-mo channels under no voltage; (b) Fluorescence spectra of probe molecule (phenol) transport in Gly-mo channels under (2V); (c) Linear relationship of phenol permeation and transport at the maximum absorption peak (298 nm).

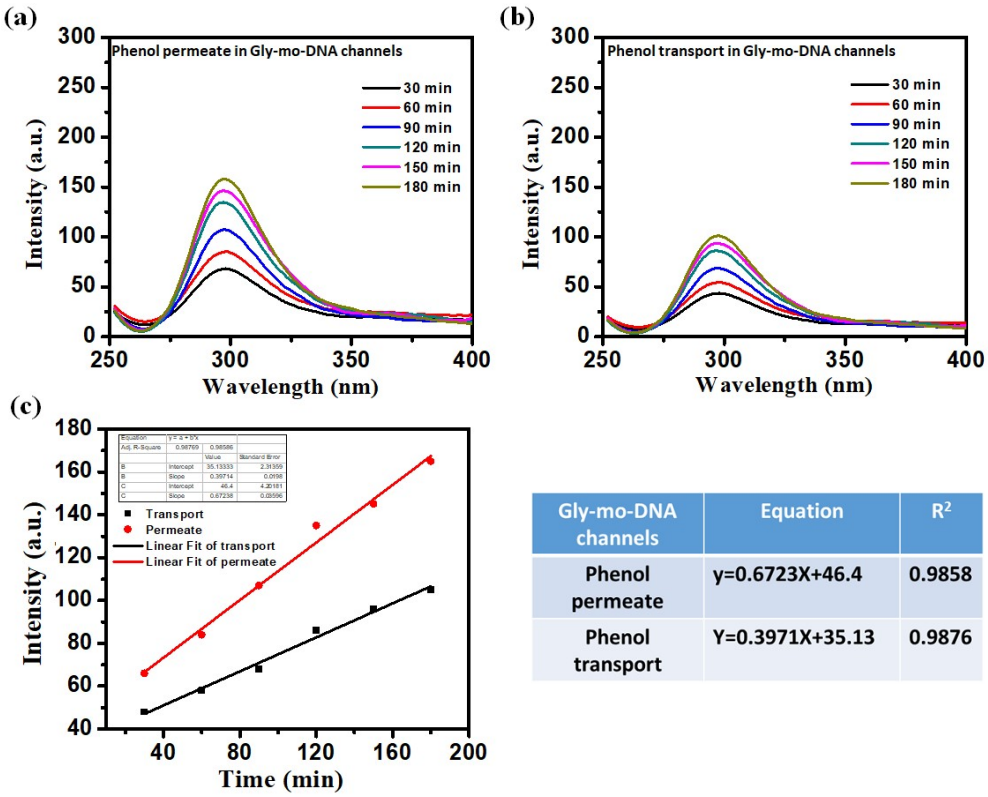

Gly-mo-DNA channels	Equation	R^2
Phenol permeate	y=0.6723X+46.4	0.9858
Phenol transport	Y=0.3971X+35.13	0.9876

Figure S26. (a) Fluorescence spectra of probe molecule (phenol) permeation in Gly-mo-ss DNA channels under no voltage; (b) Fluorescence spectra of probe molecule (phenol) transport in Gly-mo-ss DNA channels under (2V); (c) Linear relationship of phenol permeation and transport at the maximum absorption peak (298 nm).

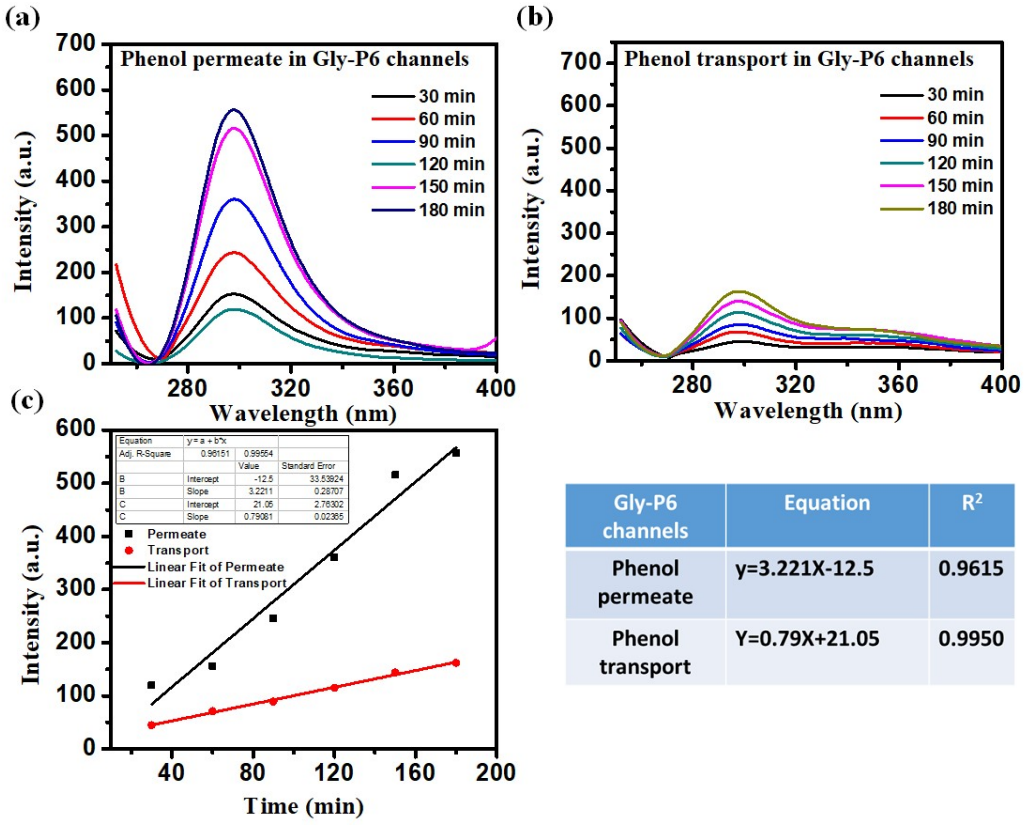

Gly-P6 channels	Equation	R^2
Phenol permeate	y=3.221X-12.5	0.9615
Phenol transport	Y=0.79X+21.05	0.9950

Figure S27. (a) Fluorescence spectra of probe molecule (phenol) permeation in Gly-P6 channels under no voltage; (b) Fluorescence spectra of probe molecule (phenol) transport in Gly-P6 channels under (2V); (c) Linear relationship of phenol permeation and transport at the maximum absorption peak (298 nm).

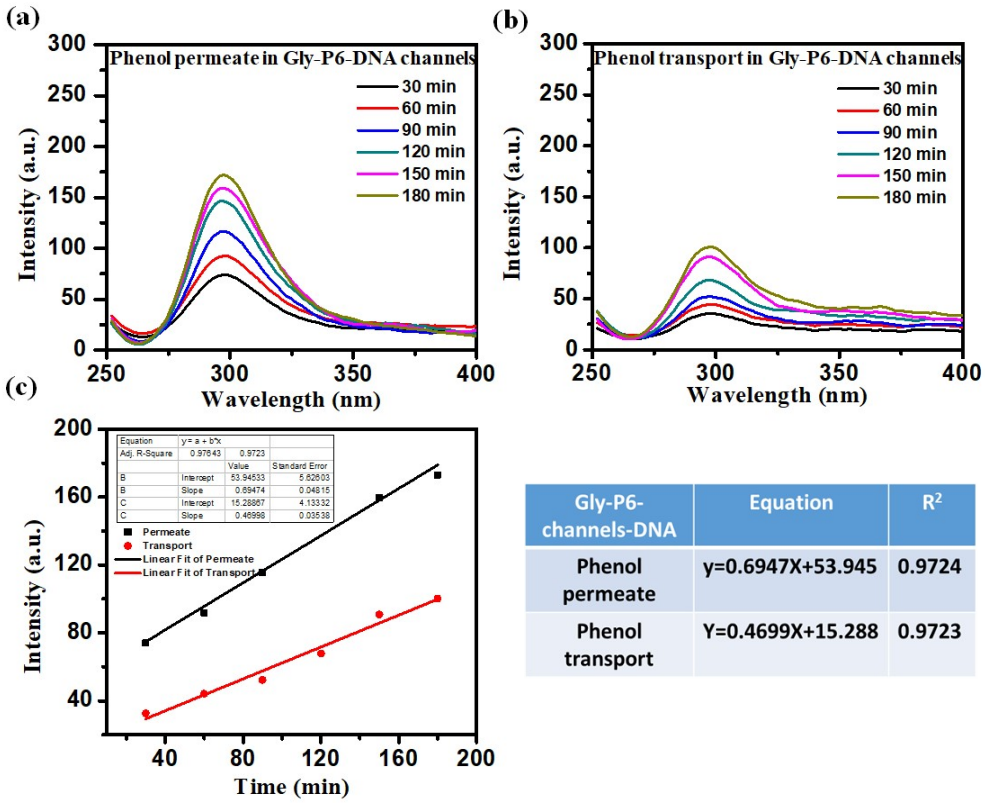

Gly-P6-channels-DNA	Equation	R^2
Phenol permeate	y=0.6947X+53.945	0.9724
Phenol transport	Y=0.4699X+15.288	0.9723

Figure S28. (a) Fluorescence spectra of probe molecule (phenol) permeation in Gly-P6-ss DNA channels under no voltage; (b) Fluorescence spectra of probe molecule (phenol) transport in Gly-P6-ss DNA channels under (2V); (c) Linear relationship of phenol permeation and transport at the maximum absorption peak (298 nm).

Table S4. The surface charge density and related parameters of the channels are calculated by EOF

Channnels	σ (e-/nm^2)	ξ (mV)	Veof (cm.s^{-1})	E(N_i/N_{diff})
Gly-mo	7.89×10^{-4}	0.6068	-9.64×10^{-3}	0.486
Gly-mo-DNA	5.92×10^{-4}	0.4555	-7.24×10^{-3}	0.5906
Gly-P6	2.63×10^{-3}	2.0227	1.75×10^{-2}	0.2455
Gly-P6-DNA	6.15×10^{-4}	0.473	-5.47×10^{-3}	0.6764

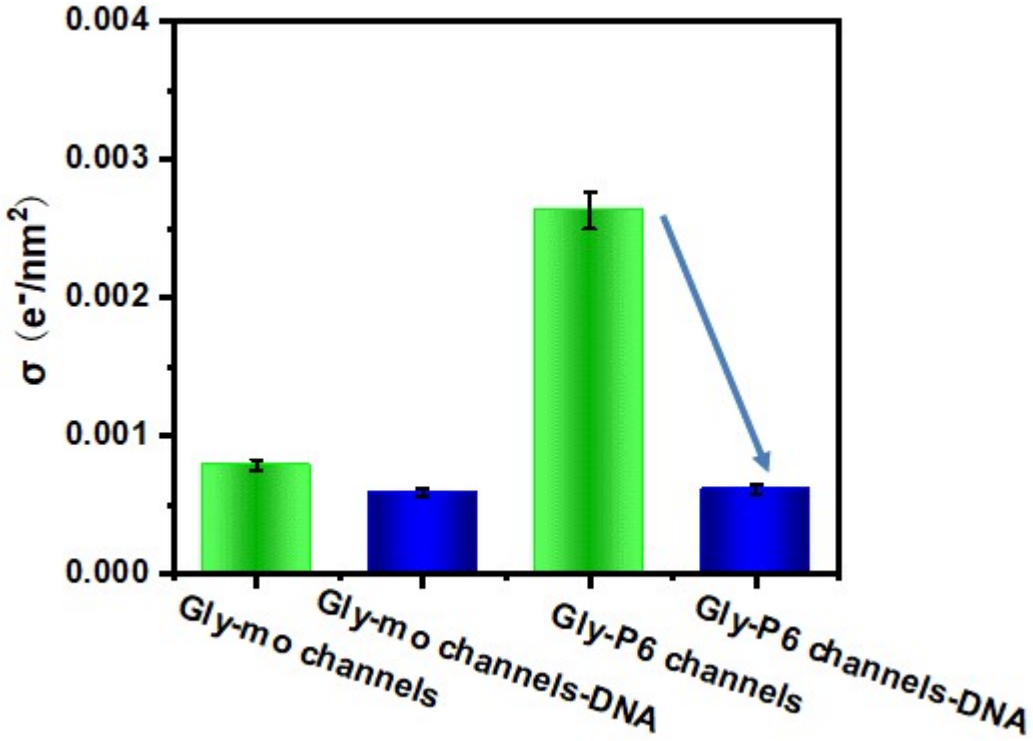

Figure S29.The histogram of surface charge density of different states of nanochannels

24. COMSOL simulation

According to the electroosmotic flow experiment, we calculated the surface charge density of the two channels. According to the calculated surface charge density, it was substituted into a specific multiphysics field, and the simulation (COMSOL Muitiphysics) software was used to theoretically simulate the ss DNA concentration distribution in the nanochannels. First, according to the thickness of the membrane and the diameter of the large and small ends, draw a two-dimensional planar geometric model of the nanochannels, as shown in Figure S27:

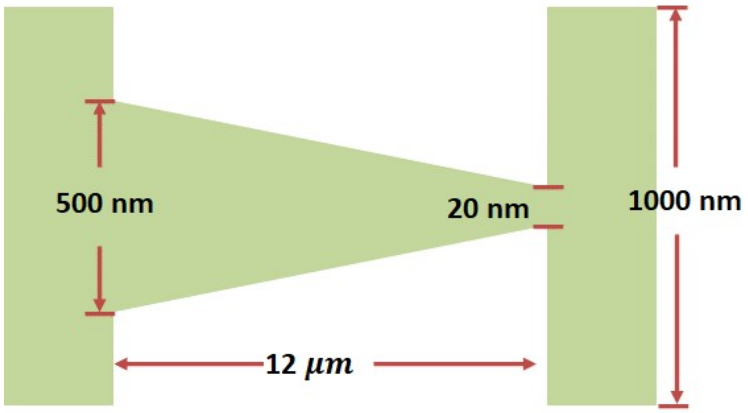

Figure 30. Schematic diagram of the plane model of the conical nanochannels Comsol simulation calculation

The simulation uses the Poisson and Nernst-Planck equations in COMSOL Multiphysics 5.3. The specific formula is as follows. Equation S5 is the Nernst-Planck equation describing the transport properties of charged channels. The electric potential and ion concentration can be expressed by Equation S6. When the system reaches a steady state, the flux should satisfy the time-independent continuity formula S7.

$$\sigma = -\frac{V_{eof}\eta}{J_{app}\rho\kappa^{-1}} \qquad S5$$

$$\Phi = -\frac{F}{\varepsilon}\sum_{i} Z_i C_i \qquad S6$$

$$J_i = -D_i\nabla C_i - \frac{FZ_i}{RT}D_i C_i\nabla\Phi + C_i u \qquad S7$$